DOI: https://doi.org/10.68732/39f17fc3f39cc3ca

ISBN: 978-9989-2053-6-1

Mobilisation of a fully grouted passive rock bolt along its length

E. Le Guidec
Univ Gustave Eiffel, Univ Lyon, GERS-RRO, Lyon, France
elise.le-guidec@developpement-durable.gouv.fr

C. Gbewade
Cerema, Bron, France
0009-0003-3240-8844

Y. Fargier
Univ Gustave Eiffel, Univ Lyon, GERS-RRO, Lyon, France
0000-0003-1139-6461

M. Bost
Univ Gustave Eiffel, Univ Lyon, GERS-RRO, Lyon, France
Cerema, Bron, France
0000-0003-0452-5931

Abstract

The ageing of hydraulic structures and the reassessment of flood parameters in light of regulatory, technical, and climatic changes are increasing the need for rehabilitation. When the theoretical stability of a structure can no longer be assured, particularly in extreme flood events, one of the reinforcement techniques considered is the use of fully grouted passive rock bolts. Groups of bolts with varying inclination angles could be set in order to withstand the two load directions causing the dam to fail by sliding or tilting. The group effect therefore must be studied through the comparison of the contribution of an isolated bolt with that of a group of bolts, and through the definition of the bolt configurations inducing this effect. This contribution depends on the mobilisation of the rebar and the surrounding environment. It appears relevant to isolate the rebar and analyse its mobilisation in order to subsequently study different configurations.

The aim of this study is therefore to characterise the mobilisation of the rebar along its length.

To achieve this, a large-scale direct shear test is carried out under constant normal stress. The mobilisation all along the rebar is monitored by optical fibre during the test. A finite element model is developed so that rebar mobilisation can be compared considering both numerical and experimental results. The validated numerical model will enable the group effect to be later studied.

Keywords

Untensioned rockbolts, Optical fibre, Finite element model, Dam reinforcement, Shear mobilisation.

1 Introduction

Rock bolting is a widely adopted technique in underground engineering and rock-slope stabilisation, and it is now being considered for the reinforcement of gravity dams (Coubard and Morel 2025), with one or several bolt rows crossing the concrete-rock interface. Configurations involving multiple rows of bolts are particularly complex, as the bolts may not mobilise simultaneously, particularly in the early stages of loading (Ferrero 1997).

For single bolts, analytical models predict that the bolt should exhibit two inflection points symmetrically located around the interface (Panet 1987; Pellet 1993). Previous experimental studies using strain gauges have characterised bolt mobilisation (Ferrero 1995; Mazzoleni and Richard 1998; Grasselli 2005; Jalalifar et al. 2006), but these measurements are limited to discrete points. Distributed optical sensing techniques have been introduced to address this limitation and tested on non-grouted rebars or on double-shear tests (Hyett et al. 2013; Forbes et al. 2017).

To gain insight into the collective behaviour of bolts reinforcing a sheared interface, we propose in this paper an innovative approach to characterise the rebar mobilisation so that it can later be distinguished from the overall response, which also includes changes in the mobilisation of the reinforced interface. This approach combines a dedicated numerical model, a large-scale experimental setup instrumented with innovative optical sensing techniques, and a derivation method to extract force resultants.

First, a large-scale direct shear test is presented evaluating the performance of optical fibre sensing for measuring the mobilisation of a bolt reinforcing a sheared concrete-concrete interface. Then, after presenting the experimental setup and a first finite element model, the bolt mobilisation along its length, as measured by optical fibre and calculated in the model, is discussed through a comparison of numerical and experimental results and through a derivation of force resultants.

2 Experimental Setup

The experiment is carried out using an exceptional device based on the Casagrande shear box concept but of large dimensions (1 m x 1.5 m shear surface) (Bidaut et al. 2006; Mazzoleni and Richard 1998). The upper box moves horizontally relative to the fixed lower box thanks to horizontal cylinders; transverse motion is restrained, while rotation of the upper box is permitted.

The purpose of this first test is to evaluate the instrumentation setup and gain a better understanding of the stress distribution along the length of a rock bolt. The test conditions are for this experiment not dam-specific. The test specimen consisted of prefabricated C40/50 concrete blocks. A 65-mm-diameter grooved steel cylindrical sleeve, inclined at 60° to the shear direction, is incorporated before casting. A 28-mm SAS 500 threaded rebar is subsequently installed inside this sleeve and grouted with a cementitious mortar (compressive strength: 33.4 MPa).

A constant normal load of 994 kN is applied by two hydraulic cylinders attached to a frame that followed the motion of the upper block, thereby maintaining normality of the applied load. Tangential displacement is imposed at a rate of 1 mm/min using horizontal cylinders with a maximum capacity of 5 MN. In order to isolate the influence of the bolt, a preliminary shear test without bolt is conducted before grouting.

The rebar is instrumented using a jacketed optical fibre bonded inside a groove running around the rebar, following a configuration similar to that of Forbes et al. (2017). In order to have only one fibre to interrogate, the fibre loops at the end of the rebar. Distributed strain measurements are obtained every 2.6 mm at an acquisition rate of 50 Hz.

Consequently, in the following analysis, two parallel fibre sections are distinguished (Fig. 1): the first encountered in the shear direction is referred to as the “upstream fibre” and the second as the “downstream fibre”. The lower end of the downstream fibre is assumed to coincide with the lower face of the bottom block, and strain profiles are plotted from the bottom to the top of the rebar. Because the rebar is inclined, the fibre coordinate does not correspond directly to elevation, requiring careful definition of the rebar-interface intersection. The initial fibre state corresponds to the beginning of the shear phase (zero-strain reference). Missing strain data due to signal loss are linearly interpolated when fewer than four consecutive measurement intervals are affected. The strain profiles are then smoothed along the bolt length using a 1-cm moving window.

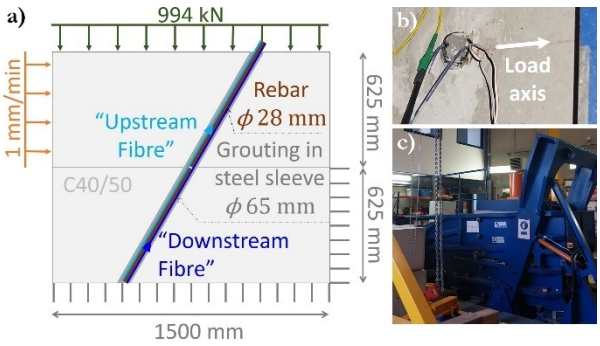


Fig. 1 Experimental setup: (a) Schematic representation of the experimental setup with the optical fibre placement relative to the loading conditions. (b) Photograph of the head of the bolt. (c) Photograph of the apparatus during test preparation.

3 Numerical model

A finite-element model is built in COMSOL v6.4. The rebar, grout, and precast blocks are explicitly modelled, but the cylindrical sleeve around the grout is not included. Interfaces between the rebar and grout, and between the grout and blocks, are assumed fully bonded. The block-to-block interface is modelled as a frictional contact with a friction coefficient of 0.75, corresponding to the measured apparent friction coefficient at 9.7 mm displacement in the preliminary shear test. All materials are treated as linear elastic and isotropic. The blocks and grout share the same concrete material properties, while the rebar is modelled as steel (Table 1). For numerical convergence, the two faces of the lower block normal to the shear direction are constrained against displacement in that direction, and vertical displacement is fixed on the bottom face. Loading is applied in two steps:

- Incremental uniform application of the normal load on the upper surface of the upper block.
- Incremental uniform application of the tangential load on the corresponding face (Fig. 1).

Table 1. Parameters used in the numerical model.

Material	Young's modulus [GPa]	Poisson's ratio [-]	Density [kg/m^3]
Concrete	38	0.2	2400
Steel	200	0.3	7800

4 Bolt mobilisation along its length

4.1 Results

In the experimental test, bolt failure occurred at a tangential displacement of 43 mm. The fibre data at the theoretical interface are presented alongside the force applied by the horizontal cylinders. Only the first 19 mm of displacement are reported here, as the optical fibre broke beyond this point (Fig. 2).

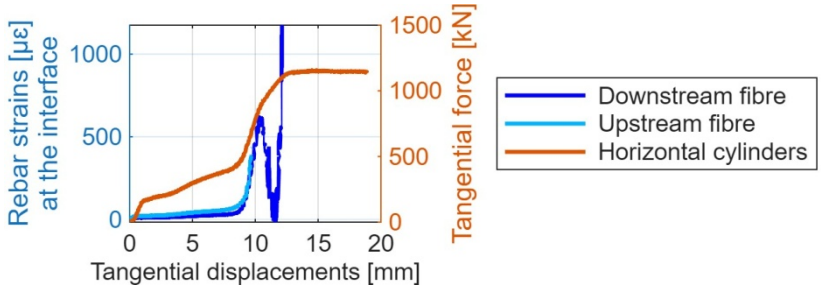


Fig. 2 Rebar strains(cyan / blue) at the theoretical interface, defined as the plane normal to the rebar axis centred at the block interface (white in Fig. 1), and tangential force from the horizontal cylinders (orange) during displacement.

The fibre sections located at the interface undergo the largest strains, which leads to significant signal distortion and early signal loss. Specifically, the upstream fibre signal is first lost at the interface once displacement reaches 9.7 mm, corresponding to a strain of 400 με (Fig. 2). The tangential force curve exhibits three distinct slopes before reaching a plateau of 1.15 MN at approximately 12.5 mm tangential displacement, which persists until bolt failure. Between 1 and 9 mm, the bolt is only lightly mobilised, consistent with the lower slope of the tangential force. After 9 mm of displacement, the bolt becomes more significantly mobilised, and this transition appears to coincide with the change in slope of the tangential force curve (Fig. 2).

Experimental (left) and numerical (right) strain profiles are compared at tangential displacements of 5, 10 and 13 mm (Fig. 3).

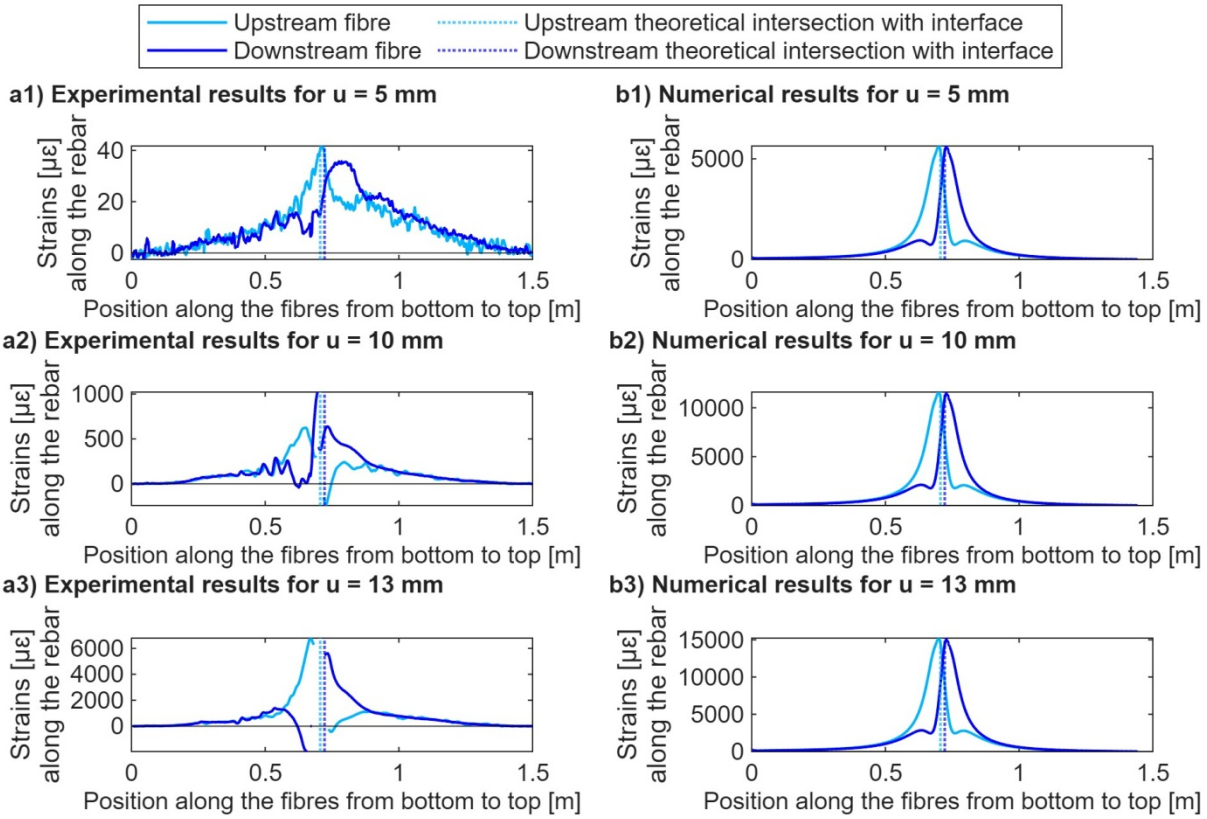


Fig. 3 Upstream (cyan) and downstream (blue) fibre-optic strain experimental (a) and numerical (b) profiles (cf Fig. 1) at 5 mm (1), 10 mm (2), and 13 mm (3) displacements (u tangential displacement of the box).

Experimental strains along the bolt (Fig. 3) increase from a maximum of 40 με at 5 mm of displacement (Fig. 3 – a1) to 8000 με at 13 mm (Fig. 3 – a3). At low levels of mobilisation, each fibre displays a single strain peak (Fig. 3 – a1), near the interface for the upstream fibre and in the upper part of the bolt for the downstream one. Starting at 9-10 mm of displacement (Fig. 3 – a2), isolated narrow peaks develop close to the theoretical intersection between the interface and the upstream fibre, quickly leading to signal loss, while two peaks appear on either side of the theoretical interface. The position of a maximum on one fibre generally corresponds to a local minimum on the other, yet their positions are asymmetric relative to the theoretical interface. With further displacement (Fig. 3 – a3), these peaks increase in amplitude and the signal remains lost in the zone adjacent to the interface.

In the numerical model (Fig. 3 – b1, b2 and b3), the bolt experiences purely tensile loading, with strain magnitudes ranging from 6000 με at 5 mm of displacement to 15000 με at 13 mm. Bolt mobilisation is concentrated within roughly the first 300 mm around the interface. The numerical strain profiles maintain a similar shape throughout shearing, with two peaks located on either side of the interface. The maximum strain on one fibre roughly coincides with a local minimum on the other.

4.2 Discussion

The approximate alignment between strain maxima and minima suggests inflection points on both sides of the interface. Experimental and numerical results show similar features, particularly at 13 mm displacement (Fig. 3 – a3 and b3), although the experimental inflection points appear more widely spaced (from 0.06 to 0.08 m versus 0.03 m in the numerical results), less centred on the theoretical interface, and less symmetric. The numerical model overestimates bolt tension, particularly at the onset of shearing (peak strain ratio of 100at 5 mm displacement, dropping to 2.5 at 13 mm).

Three modelling limitations likely explain these discrepancies. Improved representation of the concrete-concrete interface and the tilting motion of the upper block may help capture the early stages of the test more accurately. Moreover, the effect of the steel sleeve surrounding the grout, which is omitted in the numerical model, on the magnitude of the strains is not known. Nevertheless, it likely causes most of the underestimation of the spacing between inflection points: the spacing between inflection points depends on bolt diameter (Dight 1985), so adding a larger-diameter steel tube likely

increases it. Finally, accounting for grout damage and grout-rebar interaction should improve the shape and concentration of strains; for example, grout failure would promote a more progressive deformation pattern (Azuar 1977).

Assuming a Young's modulus of 200 GPa for the steel rebar, these strain results allow the calculation of stresses along the optical fibres (Fig. 4a). By treating the rebar as a compound bending beam, the normal force and bending moments along the rebar can be computed (Fig. 4b). Assuming an infinitesimal gauge spacing then allows estimation of the shear force along the rebar (Fig. 4c).

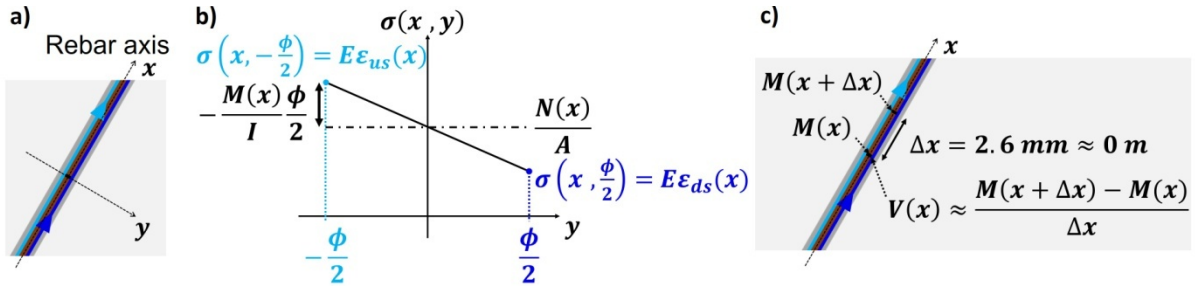


Fig. 4 Assumptions on axial stress $\sigma(x, y)$ (b) and optical fibre gauge spacing Δx(c) for computing normal force$N(x)$, moment$M(x)$, and shear force$V(x)$along the rebar axis x(a) based on strain measurements from the upstream fibre $\varepsilon_{us}(x)$ and downstream fibre $\varepsilon_{ds}(x)$, for a rebar with Young's modulus E, diameter ϕ and moment of inertia I.

The results at the theoretical interface at 9.7 mm displacement, before signal loss in the upstream fibre, show a normal force of 46 kN, a shear force of 17 kN and a bending moment of -24 N.m, near a zero-moment point (Fig. 5). The 53 kN difference between tests with and without the bolt matches the order of magnitude of fibre-optic derived force estimates. However, using this comparison to estimate bolt mobilisation is questionable, especially before the plateau of tangential-force development is reached: the bolt's contribution also depends on the bolt-induced change in interface mobilisation that occurs at the onset of shearing. The effect of the steel sleeve around the grout on mobilisation is also unknown.

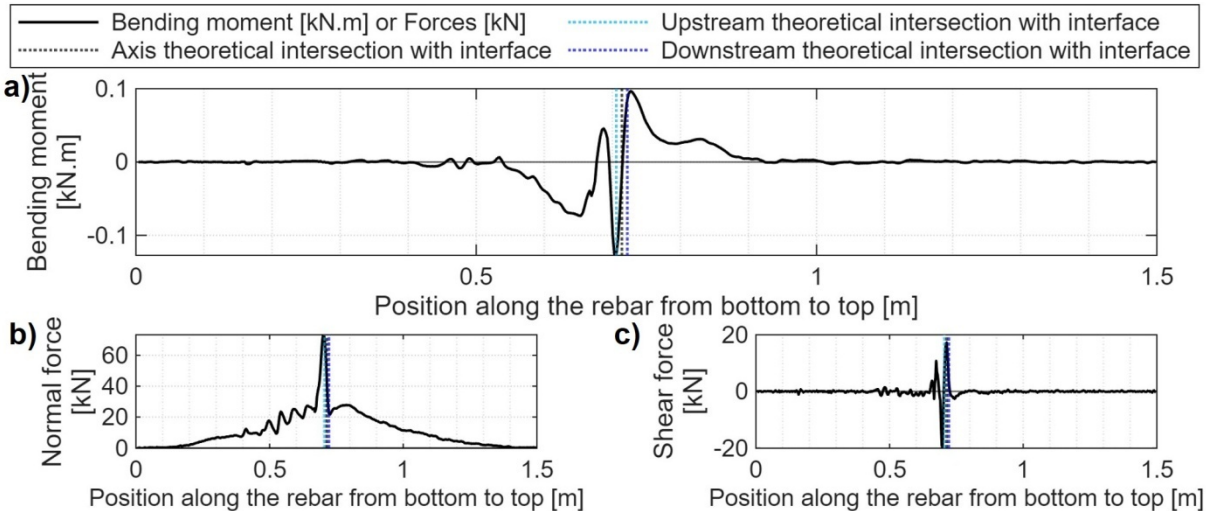


Fig. 5 Bending-moment (a), normal-force (b) and shear-force (c) profiles along the rebar at 9.7 mm displacement.

The alignment of measurement points is critical for computing forces and moments, particularly when strain varies rapidly along the bolt. The uncertainties in the position along the bar, mainly due to the measurement step size, the placement of the fibre during bonding and the end-marking of the fibres, inevitably introduce uncertainties in this alignment. Furthermore, the compound bending-beam model used here is only valid for small rotation gradients. A potential improvement would be to assess the influence of a more accurate representation of shear effects, particularly near the interface and the inflection points.

An effective comparison between these results and the overall contribution of the bolt at the given displacement requires a precise definition of the interface position. This position cannot be reliably determined in post-processing because, unlike the assumptions typically made in analytical models (Panet 1987; Pellet 1993), the point where the computed bending moment becomes zero shifts during the initial stages of loading, and it even crosses zero three times over a very short segment of the rebar for a 9.7 mm displacement (Fig. 5). This issue will be addressed in future experiments. These tests will be performed without the steel sleeve around the grout, which should reduce uncertainties.

5 Conclusion

The mobilisation of an inclined rebar during a shear test is monitored using an optical fibre and compared with numerical simulation of the test.

The optical fibre allowed continuous tracking of rebar mobilisation up to 9.7 mm of displacement, when the signal is partially lost on the upstream side, near the interface. The mobilisation of the remaining portion of the rebar which ultimately failed at 43 mm could still be followed up to 18.8 mm without fibre rupture. Based on the measured strains, axial force, shear force, and bending moment are calculated.

The two inflection points predicted by the analytical framework are clearly identifiable. However, the bending-moment profile reconstructed from the strain data shows more peaks than expected. Improving the localisation of the rebar relative to the interface will be necessary in future experiments to better understand the origin of these variations, especially if they persist in a simpler configuration without the steel sleeve around the bolt reservation.

Even so, this technique appears promising both for quantifying the contribution of bolt mobilisation at the interface during early loading and for locally calibrating numerical models, thereby refining the simplified initial model by improving the representation of the interface and the grouting. It will be applied to later experimental campaigns on group effect under a traction-compression and shear load, as encountered for dam rehabilitation.

References

Azuar JJ (1977) Stabilisation des massifs rocheux fissurés par barres d'acier scellées. Rapport de recherche LCPC n°73. Laboratoire Central des Ponts et Chaussées, Paris, France

Bidaut P, Durville JL,Guillemin P, Richard JC, Viktorovitch M (2006) Essais de cisaillement sur discontinuités rocheuses armées par ancrages passifs : Utilisation d'une boîte de cisaillement de grandes dimensions. Bulletin des Laboratoires des Ponts et Chaussées n°263-264: 7-18.

Coubard G, Morel F (2025) Reinforcement of Existing Dams with Passive Anchors: Thoughts and Proposals from a French Working Group. Twenty-Eighth International Congress on Large Dams, Chengdu, China, 2025-05-23

Dight P (1985) The theoretical behaviour of full contract bolts subject to shear and tension. The Role of Rock Mechanics in Excavations for Mining and Civil Works, International Society for Rock Mechanics, Zacatecas, Mexico, 1985-09-01.

Ferrero AM (1995) The shear strength of reinforced rock joints. International Journal of Rock Mechanics and Mining Sciences & Geomechanics Abstracts 32 (6): 595-605. 10.1016/0148-9062(95)00002-X.

Ferrero AM, Giani GP, Migliazza M, Egger P (1997) Physical and numerical analysis of reinforced rock joint behaviour. RivistaItaliana di Geotechnica 3-4: 63-89.

Forbes B, VlachopoulosN, Hyett AJ, Diederichs MS (2017) A new optical sensing technique for monitoring shear of rock bolts. Tunnelling and Underground Space Technology 66: 34-46. 10.1016/j.tust.2017.03.007.

Grasselli G (2005) 3D Behaviour of bolted rock joints: experimental and numerical study. International Journal of Rock Mechanics and Mining Sciences 42 (1): 13-24. 10.1016/j.ijrmms.2004.06.003.

Hyett A, Forbes B, Spearing S (2013) Enlightening Bolts: Using Distributed Optical Sensing to Measure the Strain Profile along Fully Grouted Rock Bolts. 32nd International Conference on Ground Control in Mining, Morgantown, WV, USA, 2013-07-30

Jalalifar H, Aziz NH, Hadi M (2006) An Assessment of Load Transfer Mechanism Using the Instrumented Bolts. 7th Underground Coal Operators' Conference, Keiraville, Australia, 2006-07-07

Mazzoleni G, Richard JC (1998) Caractéristiques de fonctionnement des ancrages passifs – Campagne d'essais 1997. FAER 2-24-14-7. Centre d'Etudes Techniques de l'Equipement, Laboratoire Régional des Ponts et Chaussée Rhône-Alpes, Bron, France

Panet M (1987) Reinforcement of rock foundations and slopes by active or passive anchors. Sixth International Congress on Rock Mechanics - Theme 2 Rock foundations and slopes, Montreal, Canada, 1987-09-01

Pellet F (1993) Résistance et déformabilité des massifs rocheux stratifiés renforcés par ancrages passifs. PhD Thesis at Ecole Polytechnique Fédérale de Lausanne